

# Superquadrics-based Object Representation of Complex Scenes from Range Images

Yan Zhang, Jeffery R. Price, and Mongi A. Abidi

IRIS Lab, Department of Electrical & Computer Engineering, the University of Tennessee,  
Knoxville, TN 37996-2100

## ABSTRACT

This paper investigates the superquadrics-based object representation of complex scenes from range images. The issues on how the recover-and-select algorithm is incorporated to handle complex scenes containing background and multiple occluded objects are addressed respectively. For images containing backgrounds, the raw image is first coarsely segmented using the scan-line grouping technique. An area threshold is then taken to remove the backgrounds while keeping all the objects. After this pre-segmentation, the recover-and-select algorithm is applied to recover superquadric (SQ) models. For images containing multiple occluded objects, a circle-view strategy is taken to recover complete SQ models from range images in multiple views. First, a view path is planned as a circle around the objects, on which images are taken approximately every 45 degrees. Next, SQ models are recovered from each single-view range image. Finally, the SQ models from multiple views are registered and integrated. These approaches are tested on synthetic range images. Experimental results show that accurate and complete SQ models are recovered from complex scenes using our strategies. Moreover, the approach handling background problems is insensitive to the pre-segmentation error.

**Keywords:** Superquadrics, Object representation, Segmentation, Range image

## 1. INTRODUCTION

Automatically detecting and describing complex objects is an important goal in the computer vision area. It is indispensable in many visual tasks including generic object recognition, navigation, robotic manipulation, and object learning. The shape of an object can be represented by three levels of primitives as respect to the dimensional complexity: volumetric primitives, surface elements, and contours. As the highest-level representation, volumetric primitives represent the most intuitive decomposition of an object into parts. Models composed of volumetric primitives can easily support part articulation and, at the structural level, are insensitive to dimensional changes in the parts. These part-level characteristics enable volumetric primitives to support object manipulation, functional-based object recognition, and other high-level activities. The most commonly used volumetric primitives include generalized cylinders, geons, and superquadrics. Among these different volumetric primitives, superquadric representation has received substantial attentions due to its own advantages of recovery and rendering, and on the other hand, insolvable problems caused by the recovery of generalized cylinders. As a subclass of generalized cylinders, superquadrics are a family of geometric solids, which can be interpreted as a generalization of basic quadric surfaces and solids. With only a few parameters, they can represent a large variety of regular geometric shapes. This makes superquadrics much more convenient for object representation.

The problem of direct recovery of individual superquadrics from range images was first solved by Solina and Bajcsy.<sup>9</sup> They presented an error metric combining the inside-outside function of superquadrics and a volume constraint. In their paper, Levenberg-Marquardt method was used to minimize the objective function. Ferrie, Lagarde, and Whaite<sup>4</sup> proposed a bottom-up strategy based on sequential application of different techniques to extract image regions corresponding to convex volumetric parts. They used Darboux frames to describe object surfaces and snake contour models to interpolate between image features that partition the object surfaces into its constituent parts. Leonardis and Gupta<sup>7,8</sup> used a recover-and-select paradigm to recover superquadric models of articulated objects from unsegmented range images. The main advantage of this classify-and-fit approach is that

---

Further author information: (Send correspondence to Yan Zhang)

Yan Zhang: E-mail: yzhang5@utk.edu

the performance of fitting is constantly monitored. Jaklić<sup>6</sup> refined the recover-and-select algorithm and extended this approach to recover superquadric models from multi-view range images. Recently, Zhou and Kambhamettu<sup>11</sup> extended superquadrics by introducing exponential functions to model more complicated non-symmetric objects.

Though considerable work has been done in superquadric representation, there exists some weaknesses in current systems. No prior work has addressed superquadric representation of complex scenes or handled it very well. For range images containing background, Van Dop<sup>3</sup> and other researchers stated that a simple thresholding could remove background and keep objects in an image. However, this strategy works only for even and simple background. In the presence of some complex backgrounds such as a linked wall and floor as shown in Fig. 2, the simple thresholding can not remove all the background correctly. On the other hand, for range images including multiple occluded objects, superquadric representation in a single view may not represent objects completely due to the incomplete visible information caused by occlusion. Jaklić<sup>6</sup> concluded superquadric representation was robust to view changes, and superquadric models recovered from a single view are complete and accurate enough, but it is not true when occlusions between objects are serious as shown in Fig. 8. No prior work has treated this problem. In Ref. 10, a few data sets from multiple views are first registered and fused. Next, the new data set was used to recover geons. This approach requires accurate information about camera locations, which is not accessible in some cases. Furthermore, the registration based on raw data requires heavy overlapping between views, which is unnecessary in volumetric primitive-based representation.

In this paper, we investigate superquadric representation of complex scenes from range images. The issues on how the recover-and-select algorithm<sup>8</sup> is incorporated to handle complex scenes containing background and multiple occluded objects are addressed respectively. Tasks involving such as superquadric model registration and integration are discussed as well.

The remainder of the paper is organized as follows. In section 2, we briefly explain superquadric representation of simple scenes. Superquadric representation of complex scenes is proposed in section 3. Experimental results on synthetic range images are shown in section 4. Finally, conclusions and future work are presented in section 5.

## 2. SUPERQUADRIC REPRESENTATION OF SIMPLE SCENES

In this section, we briefly introduce superquadric representation of simple scenes. In contrast to complex scenes, simple scenes assume that only even background, single-part objects, or multi-part objects without serious occlusion are included in images, or they are simply well pre-segmented images containing only objects. In such cases, superquadric model recovery is very straight forward. For images containing even background, a simple thresholding operation can remove the background. For the multi-part objects without serious occlusion, superquadric model, as a volumetric primitive, can handle self-occlusions. In such cases, an image from a single view can provide sufficient information to complete and accurate representation.

### 2.1. Superquadric Representation

Superquadrics are a set of geometric shapes generalized from basic quadric surfaces and solids. With a few parameters, they can represent a large variety of geometric shapes such as cylinders and boxes. A superquadric surface is defined implicitly by the following equation:

$$F(x, y, z) \equiv \left[ \left( \frac{x}{a_1} \right)^{\frac{2}{\varepsilon_2}} + \left( \frac{y}{a_2} \right)^{\frac{2}{\varepsilon_2}} \right]^{\frac{\varepsilon_1}{2}} + \left( \frac{z}{a_3} \right)^{\frac{2}{\varepsilon_1}} = 1 \quad (1)$$

where  $a_1, a_2, a_3$  define the size of superquadrics in the x, y and z directions,  $\varepsilon_1, \varepsilon_2$  define the changing shapes.

To recover a superquadric model in a general position, 11 parameters need to be recovered in the implicit definition of superquadrics

$$F(x_w, y_w, z_w) = F(x_w, y_w, z_w; a_1, a_2, a_3, \varepsilon_1, \varepsilon_2, \phi, \theta, \psi, p_x, p_y, p_z) \quad (2)$$

where  $\phi, \theta, \psi$  define the orientation, and  $p_x, p_y, p_z$  the position in space. We refer to the set of these parameters as  $\Lambda = \{a_1, a_2, a_3, \varepsilon_1, \varepsilon_2, \phi, \theta, \psi, p_x, p_y, p_z\}$ .

Superquadric model recovery is essentially a data fitting process. An objective function is needed to measure how well the model fits the data as an error metric. Since global minimization is extremely time consuming and complicated to implement, most researchers use local minimization methods to do the "good-fitting" instead of

the “best-fitting” achieved by global minimization. The objective function proposed by Solina<sup>9</sup> is one of the most commonly used, and it is expressed in the following equation:

$$G_1(\Lambda) = a_1 a_2 a_3 \sum_{i=1}^N (F^{e_1}(x_c, y_c, z_c) - 1)^2 \quad (3)$$

where  $x_c, y_c, z_c$  is the coordinate of a point in the canonical system. The item  $a_1 a_2 a_3$  is positively proportional to the volume which leads to the resulting superquadrics to fit the data and has minimum volume as well.

The Levenberg-Marquardt method is commonly used to solve the nonlinear least-square optimization problem, i.e., the minimization of the objective function.

## 2.2. Recover-and-Select Algorithm

The recover-and-select paradigm<sup>8</sup> is proposed to recover multiple articulated objects automatically. It consists of two interactive model-recovery and model-selection stages. In the model recovery stage, seeds placed in the whole objects are grown into models iteratively. In the model selection stage, all the redundant models are selected to fulfill the simplest description based on MDL (minimum description length) principle. This interleaving scheme has a lot of advantages over the early work in superquadric representation. First, it does not need any low-level information including edges and surfaces. Second, it does not need any prior information about cameras or objects to be represented. It can also recover correct multi-part superquadric models from complicated objects automatically. However, the images tested in their work contain no complex background nor occlusions among multiple objects, hence, they are considered as simple scenes. To represent objects in complex scenes, extra work needs to be added. This will be addressed in the following sections.

## 3. SUPERQUADRIC REPRESENTATION OF COMPLEX SCENES

In this section, a system framework is designed to recover superquadric models from complex scenes. Superquadric representation of range images containing background and multiple occluded objects are investigated respectively.

### 3.1. System Framework

A system framework to represent objects in complex scenes is shown in Fig. 1. In this system, input is a single-view range image of a complex scene. Three Dimensional superquadric models based on recovered parameters are visualized as output. In the case that an image includes a complex background, a coarse pre-segmentation is needed to remove the background. In the case that recovered representation is not satisfactory, multi-view information must be incorporated.

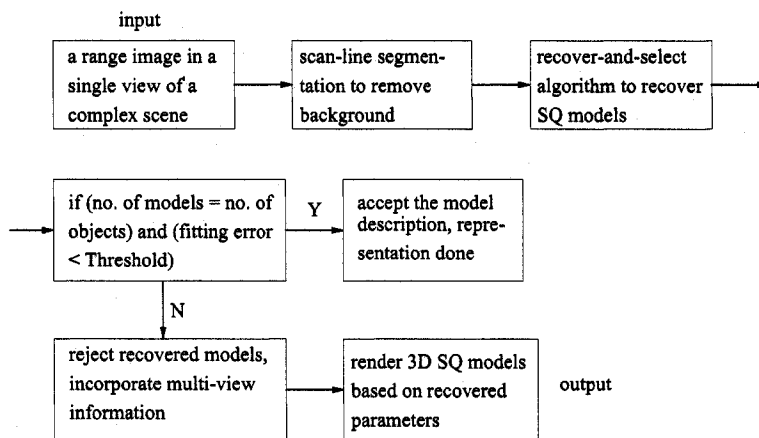
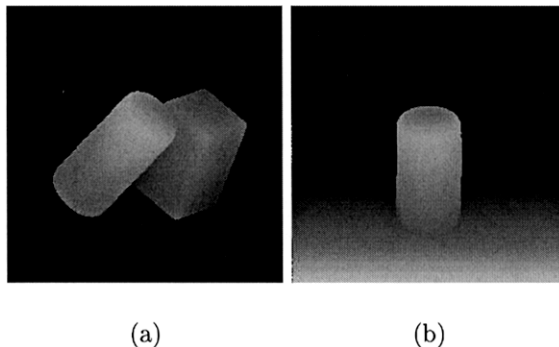


Figure 1. System framework of superquadric representation of complex scenes in a single view.

### 3.2. Range Images Containing Backgrounds: Pre-segmentation

The recover-and-select algorithm has shown excellent performance on simple range images without including background or occluded objects, however, additional work is needed to handle complex scenes. For images with background, only objects need to be represented, the problem is essentially how to remove the background while keeping objects. Most work on superquadric representation assumes that the input data has been well pre-segmented and only objects are left to be recovered. No work clearly explained how to remove backgrounds. Fig. 2 shows two range images containing a complex background. For the image in Fig. 2 (b), a simple thresholding can not remove all the backgrounds.



**Figure 2.** Synthetic range images containing backgrounds (a) a range image containing an even background (b) a range image containing a wall and a floor.

As shown in Fig. 1, our strategy includes first, a single-view range image containing background is coarsely segmented via a modified scan-line grouping segmentation approach.<sup>12</sup> An area threshold is then used to remove the background. Next, the recover-and-select algorithm is performed on the segmented image to recover superquadric models. If the representation result is satisfactory, which depends on tasks involved and system requirements, the representation is accepted and the 3D superquadric models are rendered based on recovered parameters. Otherwise, the representation is rejected. This indicates that the single-view information is insufficient to recover complete and accurate superquadric models. Therefore, additional information from other views must be incorporated. This is where the multi-view superquadric representation lies.

### 3.3. Range Images Containing Multiple Occluded Objects: Multi-view Representation

#### 3.3.1. Framework

In the case of occlusions or self-occlusions occurring in an image, the representation in a single view has low confidence due to incomplete visible data. Additional information from other views must be introduced. A multi-view representation system, as shown in Fig. 3, is constructed to obtain more convincing superquadric models.

#### 3.3.2. Circle-View Strategy

In this framework, to avoid involving the next-best-view problem, a circle-view path is designed to take images from multiple views so that we can concentrate on the multi-view representation instead of the view planning. As shown in Fig. 4, the view path is planned as a circle around the objects and images are taken approximately every  $45^\circ$  on the view path. The second view is taken in the opposite position to the first view to remove the most ambiguity while introducing the least overlapping. The third and fourth views are taken in the same rule.

#### 3.3.3. Model Registration and Integration

After all the images from multiple views are taken, superquadric models are recovered from range images in each view. The representations are sorted in a descending order according to the number of models and the fitting errors (i.e. the representation which has the most models and smallest fitting error is arranged as SQ1, SQ2, ..., etc). Next,

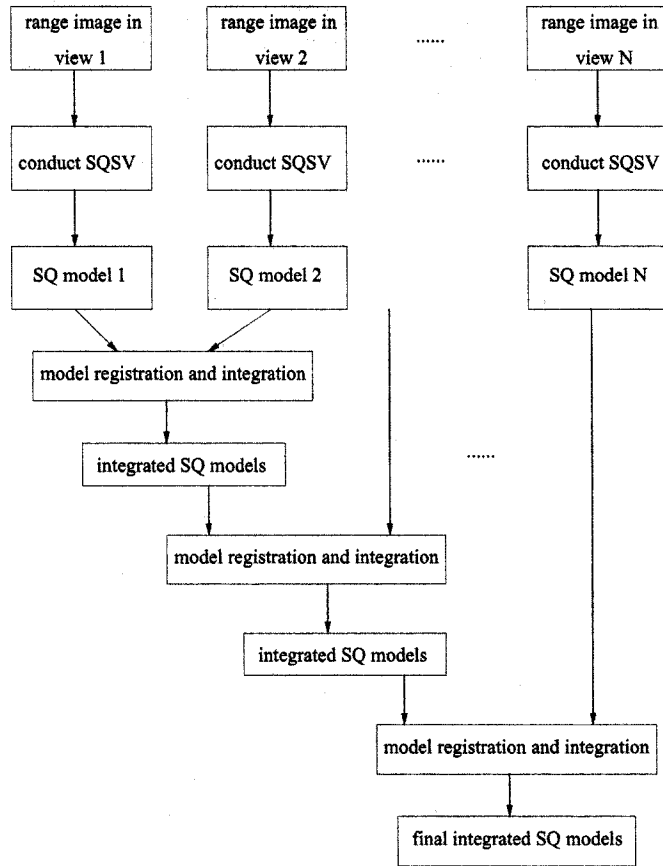


**Figure 3.** System framework of multi-view superquadric representation of complex scenes.

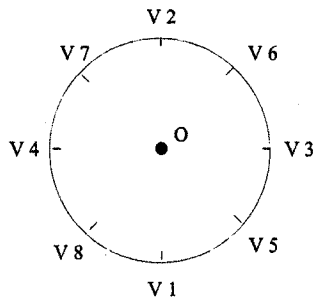


**Figure 4.** Circle-view strategy to take images from eight views: V1 is view 1, etc.

the first two representations are registered based on the parameters of recovered models using the method proposed in Ref.6. However, how to select the correct one from the four transformations calculated in the registration step, how to decide Correspondent models, and how to integrate the models recovered from multiple views were not discussed in their work. These issues will be addressed in the following.

Assume that there are SQ descriptions  $D_{11}$  and  $D_{12}$  in the first image, and descriptions  $D_{21}$  and  $D_{22}$  in the second image.  $D_{11}$  consists of region  $R_{11}$  and SQ model  $M_{11}$ ,  $D_{12}$  consists of region  $R_{12}$  and SQ model  $M_{12}$ ,  $D_{21}$  consists of region  $R_{21}$  and SQ model  $M_{21}$ , and  $D_{22}$  consists of region  $R_{22}$  and SQ model  $M_{22}$ . The following is how to decide

the correct transformation and the corresponding descriptions between the two images. The four transformations  $T_1, T_2, T_3, T_4$  have been calculated.

For every transformation  $T_i$ , first keep the representation of image 1 unchanged and transform the representation in image 2 back to image 1. For the two models in the first image, the registration errors  $E_{ij}$  are evaluated as follows

$$\begin{aligned}
E_{11} &= \sum_{x \in T(R_{21})} d(x, M_{11}) \\
E_{12} &= \sum_{x \in T(R_{22})} d(x, M_{11}) \\
E_{13} &= \sum_{x \in T(R_{21})} d(x, M_{12}) \\
E_{14} &= \sum_{x \in T(R_{22})} d(x, M_{12}) \\
E_a &= \min(E_{11}, E_{12}) \\
E_b &= \min(E_{13}, E_{14}) \\
E_1 &= E_a + E_b
\end{aligned} \tag{4}$$

where  $d(x, M_{ij})$  is the distance between the point  $x$  and the model  $M_{ij}$ .

Similarly, keep the representation of image 2 unchanged and transform the representation in image 1 to image 2. For the two models in image 2, the four registration errors are evaluated from the following equations

$$\begin{aligned}
E_{21} &= \sum_{y \in T(R_{11})} d(y, M_{21}) \\
E_{22} &= \sum_{y \in T(R_{12})} d(y, M_{21}) \\
E_{23} &= \sum_{y \in T(R_{11})} d(y, M_{22}) \\
E_{24} &= \sum_{y \in T(R_{12})} d(y, M_{22}) \\
E_a &= \min(E_{21}, E_{22}) \\
E_b &= \min(E_{23}, E_{24}) \\
E_2 &= E_a + E_b
\end{aligned} \tag{5}$$

Therefore, two registration errors ( $E_1, E_2$ ) are obtained for each transformation. For the correct transformation,  $E_1$  should be very close to  $E_2$  and they should both be less than the threshold  $E_r$ . Conducting these evaluations for all the four transformations, the transformation  $T$  with the minimal registration error, which is less than the threshold  $E_r$  is determined as the correct one. Meanwhile, the correspondent descriptions are determined by

$$\begin{aligned}
&\text{if } E_{11} < E_{12} \text{ and } E_{21} < E_{22}, \text{ then } D_{11} \text{ is correspondent to } D_{21} \text{ and } D_{12} \text{ to } D_{22} \\
&\text{else } D_{11} \text{ is correspondent to } D_{22} \text{ and } D_{12} \text{ to } D_{21}
\end{aligned} \tag{6}$$

After determining the correspondent models in the two images, the correspondent models are integrated to derive the more convincing models. In the model integration step, the parameter confidences are assigned to each model according to their fitting errors. Next, the recovered parameters of the correspondent models are combined with each other using their different confidences.

In the same manner, this integrated representation is registered with the third one to obtain another integrated representation. This procedure can be conducted until the integrated representation is satisfactory. As a result,

the multi-view representation scheme obtains the best representation with the least amount of registration and integration.

Note that this multi-view representation system is flexible and does not require all the eight views exactly. As stated in Fig. 1, only if either the recovered SQ model is not accurate enough or some objects are missing is an additional view needed. As long as satisfactory results are obtained, the task is completed. The number of views required to be taken, and when to terminate the registration and integration, heavily depend on tasks involved and system requirements.

#### 4. EXPERIMENTAL RESULTS

The proposed strategies and systems were implemented on a SGI OCTANE workstation. To test the accuracy of recovered parameters of superquadric models, synthetic range images are used in the experiments. Results on range images containing background and multiple occluded objects are shown respectively in the following sections.

##### 4.1. Results on Range Images Containing Complex Backgrounds

Experimental results on superquadric representation of range images containing complex backgrounds are shown in Fig. 5 and 6. The raw image shown in Fig. 5 contains an occluded box and cylinder with even backgrounds. Fig. 6 shows experimental results on a range image including one cylinder, a floor, and a wall as background. Correspondingly, table 1 and 2 show ground truth and recovered parameters of objects in Fig. 5 and 6. From the experimental results, we can see that our strategy is efficient to remove background and keep objects. The final recovered models are insensitive to pre-segmentation errors. Comparing to ground truth values, recovered parameters of superquadric models are accurate without affected by the background in raw images.

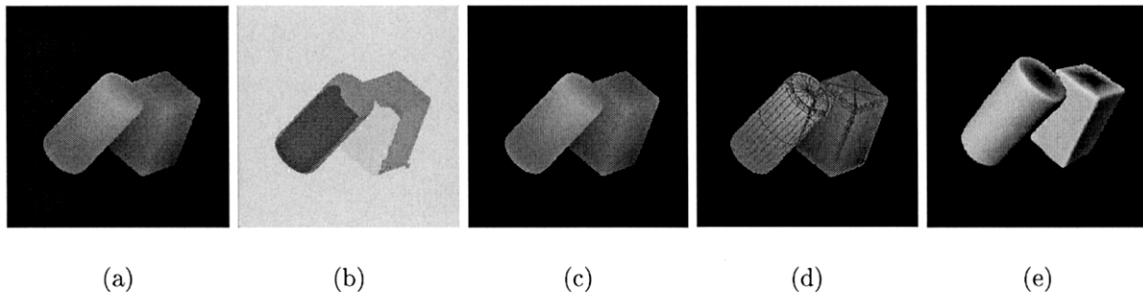


**Figure 5.** SQ representation of a synthetic range image with background. (a) input range image: 1 cylinder, 1 box with even background, (b) segmented image by scan-line grouping algorithm, (c) new image with background removed, (d) recovered SQ description: line-drawings indicate SQ wire frames, (e) reconstructed 3D SQ model from recovered parameters.

**Table 1.** Ground truth and recovered parameters of superquadric models in Fig. 5: two models are recovered, GT indicates ground truth, RP indicates recovered parameters.

Model #	P	$a_1$	$a_2$	$a_3$	$\epsilon_1$	$\epsilon_2$	$\phi$	$\theta$	$\psi$	$p_x$	$p_y$	$p_z$
1	GT	30	30	60	0.1	1.0	0.8	1.0	0	100	120	100
1	RP	27.89	29.53	58.83	0.10	1.02	0.80	1.00	0.01	99.91	118.94	102.02
2	GT	30	30	50	0.1	0.1	1.2	1.0	1.0	170	120	70
2	RP	29.46	29.82	49.83	0.10	0.10	1.20	1.00	1.00	170.33	118.79	70.05

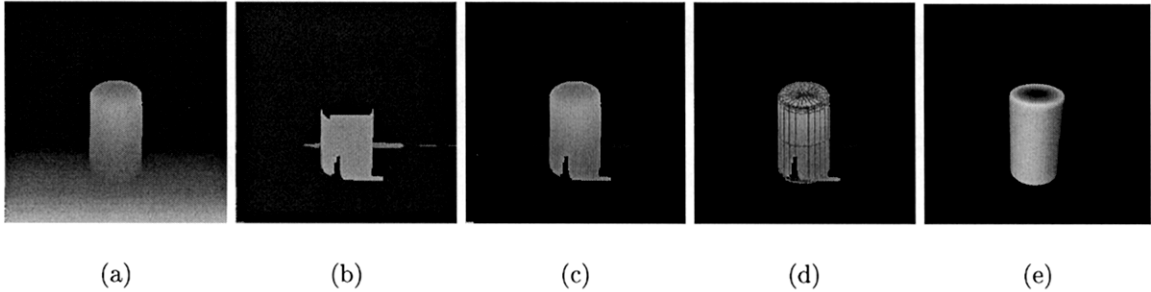


**Figure 6.** SQ representation of a synthetic range image with background. (a) input range image: 1 cylinder with a floor and a wall as background, (b) segmented image by scan-line grouping algorithm, (c) new image with background removed, (d) recovered SQ description: line-drawings indicate SQ wire frames, (e) reconstructed 3D SQ model from recovered parameters.

**Table 2.** Ground truth and recovered parameters of superquadric models in Fig. 6: one model is recovered, GT indicates ground truth, RP indicates recovered parameters.

Model #	P	$a_1$	$a_2$	$a_3$	$\varepsilon_1$	$\varepsilon_2$	$\phi$	$\theta$	$\psi$	$p_x$	$p_y$	$p_z$
1	GT	30	30	60	0.1	1.0	1.57	1.0	0	128	100	100
1	RP	29.80	28.93	52.66	0.10	1.01	1.57	1.00	0.08	127.97	104.61	104.43

## 4.2. Results on Range Images Containing Multiple Occluded Objects

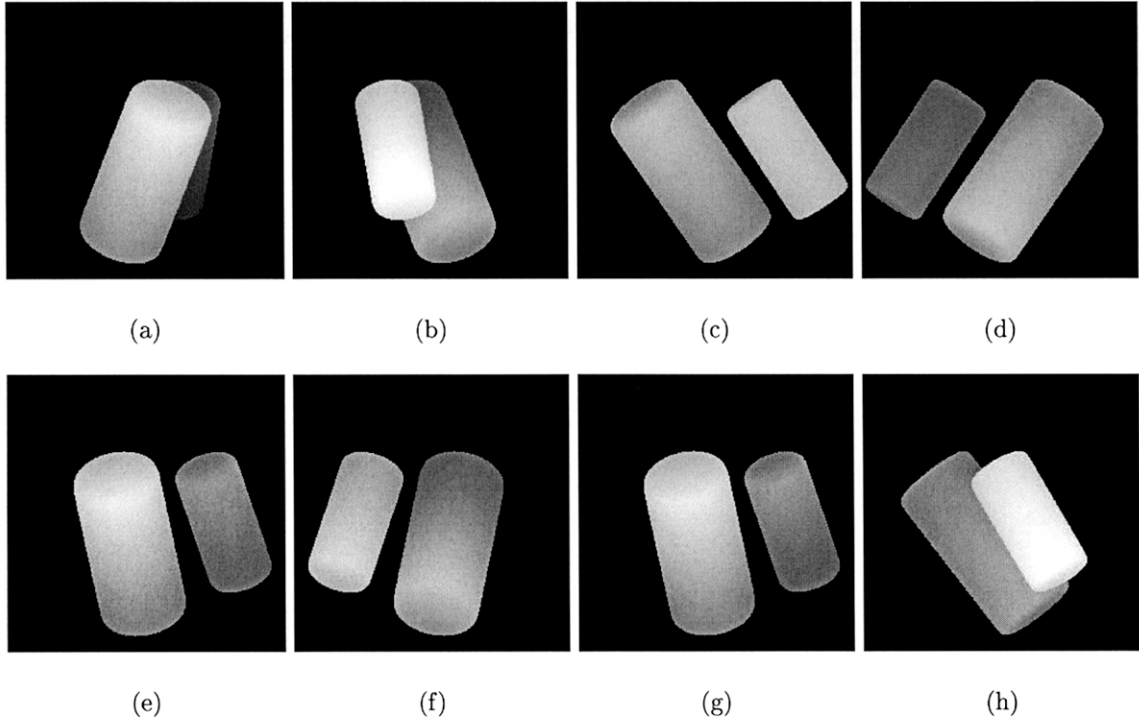
To test our multi-view representation strategy, a set of synthetic range images containing two occluded cylinders from eight different views is created using our circle-view strategy. Images are taken approximately every  $45^\circ$  on the circle around one of the objects.

Fig. 7 shows raw range images from eight views of the same scene. It is obvious that occlusions are serious in some views, but no occlusion happens in other views. The corresponding superquadric representations from view 1, view 2, and view 3 are shown in Fig. 8, 9, and 10 respectively. In Fig. 8, the smaller cylinder is missing due to serious occlusion, therefore, information from other views must be introduced to represent this missing object according to the system framework as shown in Fig. 1. Consequently, representations in views 2 and 3 are incorporated.

Fig. 11 shows registration results of the recovered superquadric models between these two views. Table 3 shows registration errors of the four transformations. The registration order affects the registration error slightly. Using the method proposed in Sect. 3.3.3, the registration errors of the four transformations shown in Fig. 11 are calculated and shown in Table 3. Based on the registration errors, the second transformation shown in Fig. 11 (b) is picked up as the correct one to align recovered models from these two views. It is calculated as

$$T = \begin{bmatrix} -0.00953806 & 0.0343751 & 0.999363 & -4.78517 \\ 0.014422 & 0.99931 & -0.0342356 & 2.63203 \\ -0.999851 & 0.0140863 & -0.0100272 & 256.311 \\ 0 & 0 & 0 & 1 \end{bmatrix}$$

The three rotation angles derived from this transformation are very close to the ground truth value:  $\phi = 0, \theta = 90^\circ, \psi = 0$ . It is also derived that model 1 in view 2 corresponds to model 1 in view 3, and model 2 in view 2 corresponds to model 2 in view 3. The confidences are assigned to each model in negative proportion to their fitting errors. Thus,



**Figure 7.** Synthetic range images of the same scene in 8 views: approximately  $45^\circ$  interval between every two images. (a) view 1, (b) view 2, (c) view 3, (d) view 4, (e) view 5, (f) view 6, (g) view 7, (h) view 8.

$$C_{12} = \frac{0.28}{0.23 + 0.28} = 0.5490$$

$$C_{13} = \frac{0.23}{0.23 + 0.28} = 0.4510$$

$$C_{22} = \frac{0.26}{0.22 + 0.26} = 0.5417$$

$$C_{23} = \frac{0.22}{0.22 + 0.26} = 0.4583$$

where  $C_{ij}$  represents the confidence of model  $i$  in view  $j$ .

The integrated parameters are calculated with these confidences as weights to the recovered parameters from single views. Table 4 shows ground truth, recovered parameters of objects from view 2, view 3, and final integrated 11 parameters from these two views.

**Table 3.** Registration errors of the four transformations in Fig. 11.

registration errors	transform 1	transform 2	transform 3	transform 4
view 2 to view 3	54.0632	3.47892	149.185	124.718
view 3 to view 2	57.916	5.10919	153.729	129.35

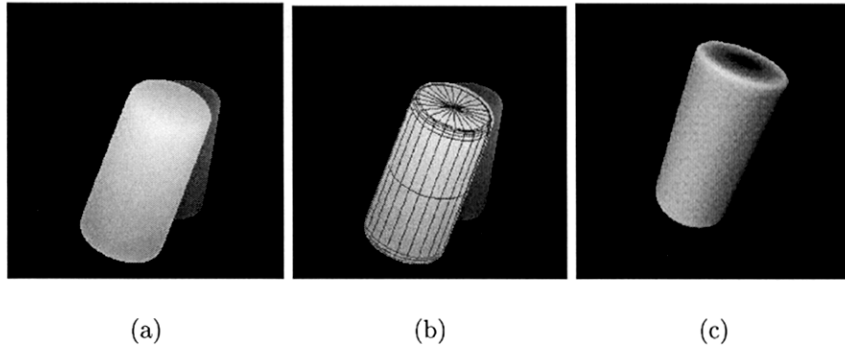


**Figure 8.** SQ representation in view 1. (a) input range image in view 1: two occluded cylinders, (b) recovered SQ description (one object is lost): line-drawings indicate SQ wire frames, (c) reconstructed 3D SQ model from recovered parameters.

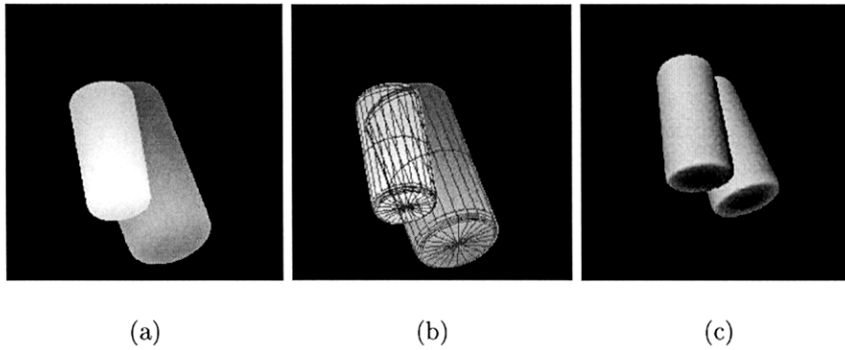


**Figure 9.** SQ representation in view 2. (a) input range image in view 2, (b) recovered SQ description: line-drawings indicate SQ wire frames, (c) reconstructed 3D SQ models from recovered parameters.

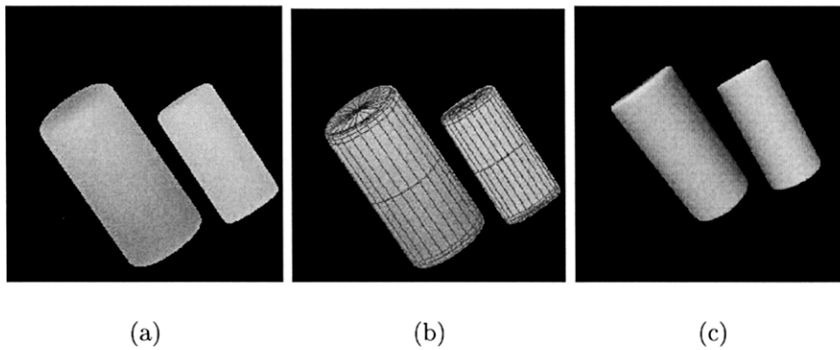


**Figure 10.** SQ representation in view 3. (a) input range image in view 2, (b) recovered SQ description: line-drawings indicate SQ wire frames, (c) reconstructed 3D SQ models from recovered parameters.

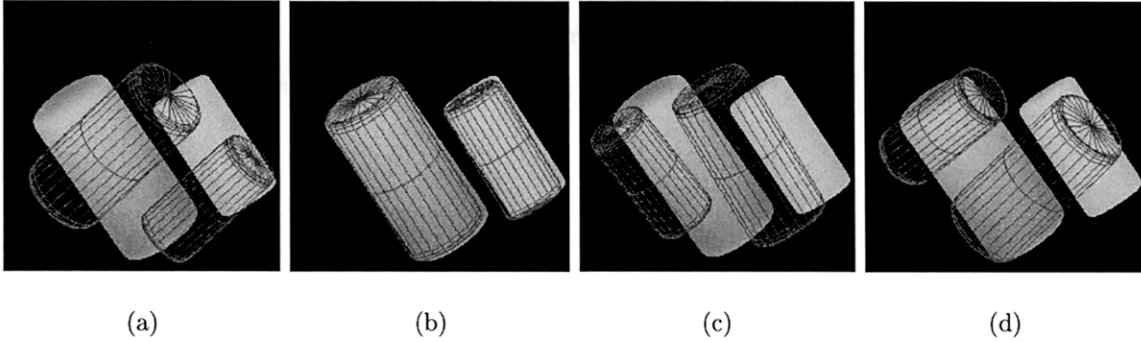


**Figure 11.** SQ registration of view 2 and view 3: keep representation in view 3 unchanged, transform representation in view 2 back according to four transformations calculated. Line-drawings indicate SQ models transformed back from view 2, background is image in view 3. (a) transform view 2 back under transformation 1, (b) transform view 2 back under transformation 2 (correct transformation), (c) transform view 2 back under transformation 3, (d) transform view 2 back under transformation 4.

**Table 4.** Ground truth and recovered parameters of superquadric models in Fig. 9 and 10: two models are recovered, GT indicates ground truth, RP indicates recovered parameters.

Model # (View)	P	$a_1$	$a_2$	$a_3$	$\varepsilon_1$	$\varepsilon_2$
1	GT	30	30	60	0.1	1.0
1 (View 2)	RP	29.76	28.81	59.40	0.1	1.01
1 (View 3)	RP	29.48	27.14	59.92	0.1	1.04
1 (Integrated)	RP	29.63	28.06	59.63	0.1	1.02
2	GT	40	40	80	0.1	1.0
2 (View 2)	RP	39.83	38.96	78.76	0.1	1.01
2 (View 3)	RP	39.71	38.29	79.81	0.1	1.02
2 (Integrated)	RP	39.78	38.65	79.24	0.1	1.01

During experiments, we found that in our case, only utilizing information in views 2 and 3 is sufficient to recover complete and accurate superquadric models from the raw image. Comparing the recovered parameters of the final integrated models with ground truth values, it is concluded that complete and accurate superquadric models are recovered from complex scenes using our multi-view representation framework.

## 5. CONCLUSIONS

In this paper, we have successfully utilized the recover-and-select algorithm into superquadric representation of complex scenes. System frameworks handling images containing complex background and multiple occluded objects are constructed respectively. The idea to extend object-based to scene-based superquadric representation enables us to explore images containing background and multiple occluded objects. Experimental results show that our strategies handle background and occlusion problems successfully. The pre-segmentation stage in our single-view superquadric representation scheme is different from those in other superquadric representation approaches. It only aims to remove background without extracting any low-level details including edges and surfaces, therefore, our strategy is robust to pre-segmentation errors. Simultaneously, our multi-view superquadric representation framework needs less views than those in multi-view surface reconstruction methods. Moreover, all the planned views are accessible due to the

2D circle path used instead of the 3D sphere.

The future work is to test our strategies on real range images. How these strategies perform on real 3D data instead of  $2\frac{1}{2}D$  range images will also be explored.

### ACKNOWLEDGMENTS

This work was supported by DOE's University Research Program in Robotics (URPR), grant number DOE-DE-FG02-86NE37968.

### REFERENCES

1. S. J. Dickinson and A. P. Pentland, "3D shape recovery using distributed aspect matching," *IEEE Transactions on Pattern Analysis and Machine Intelligence*, Vol. 14, pp. 174-198, 1992.
2. S. J. Dickinson, D. Metaxas and A. P. Pentland, "The role of model-based segmentation in the recovery of volumetric parts from range data," *IEEE Transactions on Pattern Analysis and Machine Intelligence*, Vol. 18, pp. 161-180, 1996.
3. E. Van Dop, "Multi-sensor object recognition: the case of electronics recycling", *Ph.D's thesis, University of Twente*, 1999.
4. F. P. Ferrie, J. Lagarde and P. Whaite, "Darboux frames, snakes, and super-quadratics: geometry from the bottom up", *IEEE Transactions on Pattern Analysis and Machine Intelligence*, Vol. 15, pp. 771-784, 1993.
5. A. Hoover, G. Jean-Baptiste and X. Jiang, L. Lamport, "An experimental comparison of range image segmentation algorithms," *IEEE Transactions on Pattern Analysis and Machine Intelligence*, Vol. 18, pp. 673 - 689, 1996.
6. A. Jaklic, "Construction of CAD models from range images," *Ph.D's thesis, University of Ljubljana*, 1997.
7. A. Leonardis, A. Gupta and R. Bajcsy, "Segmentation of range images as the search for geometric parametric models", *International Journal of Computer Vision*, Vol. 14, pp. 253-277, 1995.
8. A. Leonardis, A. Jaklic and F. Solina, "Superquadratics for segmentation and modeling range data", *IEEE Transactions on Pattern Analysis and Machine Intelligence*, Vol. 19, pp. 1289-1295, 1997.
9. F. Solina and R. Bajcsy, "Recovery of parametric models from range images: The case for superquadratics with global deformations", *IEEE Transactions on Pattern Analysis and Machine Intelligence*, Vol. 12, pp. 131-147, 1990.
10. K. Wu and M. Levine, "3D object representation using parametric Geons", *Technical report, McGill University*, TR-CIM-93-13, Sep, 1993.
11. L. Zhou and C. Kambhamettu, "Extending superquadratics with exponent functions: modeling and reconstruction", in *IEEE Computer Society Conference on Computer Vision and Pattern Recognition*, Vol. 2, pp. 73-78, 1999.
12. Y. Zhang, Y. Sun, J. R. Price and M. A. Abidi, "Impact of Intensity Edge Map on Segmentation of Noisy Range Images," in *Photonics West, Proc. SPIE*, Vol. 3958, pp. 260-269, 2000.